HHS Public Access

Author manuscript

Hum Genet. Author manuscript; available in PMC 2019 July 05.

Published in final edited form as:

Hum Genet. 2018 July ; 137(6-7): 447–458. doi:10.1007/s00439-018-1897-9.

IFT88 mutations identified in individuals with non-syndromic recessive retinal degeneration result in abnormal ciliogenesis.

Anil Chekuri[#1], **Aditya A. Guru**[#1], **Pooja Biswas**[#1,2], **Kari Branham**[3], **Shyamanga Borooah**[1], **Angel Soto-Hermida**[1], **Michael Hicks**[4], **Naheed W. Khan**[3], **Hiroko Matsui**[5], **Akhila Alapati**[1], **Pongali B Raghavendra**[2,6], **Susanne Roosing**[7], **Sripriya Srivatsan**[8], **Sinnakaruppan Mathavan**[8], **Amalio Telenti**[4], **John R. Heckenlively**[3], **S. Amer Riazuddin**[9], **Kelly A. Frazer**[5,10], **Paul A. Sieving**[11], and **Radha Ayyagari**[1,#]

[1]Shiley Eye Institute, University of California San Diego, La Jolla, CA, USA. [2]School of Biotechnology, REVA University, Bengaluru, Karnataka, India, [3]Ophthalmology & Visual Science, University of Michigan Kellogg Eye Center, Ann Arbor, Michigan, USA. [4]Human Longevity, Inc., San Diego, CA, USA. [5]Institute for Genomic Medicine, University of California San Diego, La Jolla, CA, USA. [6]School of Regenerative Medicine, Manipal University-MAHE, Bangalore, India. [7]Department of Human Genetics, Radboud University Nijmegen Medical Center, PO Box 9101, 6500 HB Nijmegen, Netherlands. [8]Vision Research Foundation, Sankara Nethralaya, 41, College Rd, Chennai, India [9]The Wilmer Eye Institute, Johns Hopkins University School of Medicine, Baltimore, MD USA. [10]Department of Pediatrics, Division of Genome Information Sciences, Rady Children's Hospital, San Diego, CA, USA. [11]National Eye Institute, National Institutes of Health, Bethesda, MD, USA.

[#] These authors contributed equally to this work.

Abstract

Whole genome sequencing (WGS) was performed to identify the variants responsible for inherited retinal degeneration (IRD) in a Caucasian family. Segregation analysis of selected rare variants with pathogenic potential identified a set of compound heterozygous changes p.Arg266*:c.796C>T and p.Ala568Thr:c.1702G>A in the *intraflagellar transport protein-88* (*IFT88*) gene segregating with IRD. Expression of mutant IFT88 in mIMDC3 cells by transient transfection suggested that both mutations result in the formation of abnormal ciliary structures. The introduction of the *IFT88* p.Arg266* variant in the homozygous state in HeLa cells by CRISPR-Cas9 genome-editing revealed that the mutant transcript undergoes nonsense mediated decay leading to a significant depletion of *IFT88* transcript. Additionally, abnormal ciliogenesis was observed in these cells. These observations suggest that the rare and unique combination of *IFT88*

[#] To whom correspondence should be addressed: Radha Ayyagari, PhD, Shiley Eye Institute, University of California San Diego, 9415 Campus Point Drive, JRC 206, La Jolla, CA 92093 USA, Phone: (858) 534-9029, Fax: (858) 246-0568, rayyagari@ucsd.edu.

CONFLICT OF INTEREST:

Authors declare that there is no conflict of interest.

Web link:

RetNet, http://www.sph.uth.tmc.edu/RetNet/

alleles observed in this study provide insight into the physiological role of IFT88 in humans and the likely mechanism underlying retinal pathology in the pedigree with IRD.

INTRODUCTION:

A large number of genes associated with inherited retinal degeneration have been identified (RetNet, http://www.sph.uth.tmc.edu/RetNet/). While these genes participate in a broad range of biological pathways, a substantial proportion of these genes encode ciliary proteins (Waters and Beales 2011). Cilia are evolutionarily conserved organelles that play a key role in diverse biological functions (Marshall and Nonaka 2006). Defects in ciliary structure and function are associated with several human pathologies-involving tissues in which primary cilia play a prominent role (Bisgrove and Yost 2006; Halbert et al. 1997; Pazour and Rosenbaum 2002; Wheway et al. 2014; Yoder 2007). In the retina, photoreceptor cells contain specialized ciliary structures. Photoreceptor outer segments are joined to the photoreceptor inner segments by a connecting cilium (Khanna 2015; Liu et al. 2010). Transport of proteins from the inner segment to the outer segment through the connecting cilium involves the intra-flagellar transport (IFT) machinery composed of a group of IFT proteins (Rosenbaum 2002). Mutations in genes encoding these IFT proteins lead to a set of inherited disorders known as ciliopathies, affecting several tissues including the eye, kidney and olfactory neurons (Bisgrove and Yost 2006; Waters and Beales 2011). So far, mutations in 18 IFT proteins have been implicated in IRDs (Badano et al. 2006).

Intraflagellar transport protein 88 (*IFT88*), a tetratricopeptide repeat containing protein is a core component of the IFT complex B, which is known to be involved in anterograde transport in cilia (Pazour et al. 2000). IFT complex B is required for the assembly and maintenance of primary cilia and flagella across species ranging from unicellular organisms to high-order mammals (Mizuno et al. 2012; Rosenbaum and Witman 2002). Besides its role in intraflagellary transport, *IFT88* is also involved in additional biological activities including mitosis (Delaval et al. 2011), hedgehog signaling (Chang and Serra 2013), cell migration (Boehlke et al. 2015) and cell cycle progression (Kim and Tsiokas 2011). Consistent with its multiple cellular functions, mouse models with mutant *IFT88* developed severe pathology (Lehman et al. 2008). Hypomorphic mutations in *Ift88* were reported to cause polycystic kidney disease and photoreceptor degeneration [Tg737^{orpk}] (Lehman et al. 2008; Moyer et al. 1994). *IFT88* null mutations result in embryonic lethality in mice (Murcia et al. 2000). Conditional loss of *Ift88* in the cranial neural crest cells of mice leads to craniofacial abnormalities and neonatal lethality (Tian et al. 2017). Furthermore, the ciliogenesis was observed to be abnormal in *IFT88* knock-out cell lines (Katoh et al. 2017). Based on the crucial role of this gene in development and survival, it has been long considered a candidate for various human pathologies including ciliopathies, polycystic kidney disease, photoreceptor degeneration and craniofacial abnormalities (McIntyre et al. 2012; Pazour et al. 2002; Tian et al. 2017). Thus far, mutations in *IFT88* have not been confirmed to result in human disease.

In the present study, whole genome sequence analysis (WGS) of a family identified novel compound heterozygous mutations in *IFT88* segregating with IRD. Further evaluation of the

effect of these mutations by introducing them in HeLa cells by CRISPR-Cas9 mediated genome editing and also by transiently transfecting mIMCD3 cells supported the involvement of these mutations in causing IRD and provided insight into the molecular pathology underlying IRD due to mutations in *IFT88*.

RESULTS:

Clinical analysis:

Two female siblings (Fig 1.I) of European ancestry reported impaired night vision beginning in the third and fourth decades (proband and sister). Vision impairment progressed for both, initially to mid-peripheral involvement and then to loss of central vision by the sixth and seventh decades. Patient III:I had a history of kidney stones. Her sister (patient III:II) was diagnosed with multiple sclerosis at age 43; she was also diagnosed with skin cancer and anemia, but denied any renal abnormalities. They reported no clinical or family history of other non-ocular abnormalities, including auditory disease, renal disease, craniofacial abnormalities or ciliopathy associated abnormalities. The sisters denied use of choroquine or hydroxychloroquine. Color fundus images showed marked macular neuroretinal atrophy but with some sparing of the fovea and only sparse intraretinal pigmented patches across the macular and temporal areas disproportionate to extent of RPE loss (Fig 1.II A and B). Additionally, there was only modest optic disc pallor and mild attenuation of vascular arcades.

The proband (III:I) had progressive visual acuity loss from 20/25 at age 22 to 20/125 at age 63, and the sister (III:II) progressed from 20/30 at age 37 to 20/800 at age 58. By ages 63 and 58 (proband and sister), kinetic perimetry showed bilateral dense central scotomas out to the mid-periphery but with relative retention of fields further in the periphery to a Goldman III4e target (Fig 1.II C and D).

Electroretinography was performed on both affected siblings III:I and III:II at aged 42 and 38 respectively. In proband (III:I), the response to blue and white flash under scotopic conditions was severely reduced and the b wave was delayed. The response under photopic conditions was also moderately reduced and cone response to 30Hz flicker stimulation was markedly subnormal and delayed. In her younger sister (III:II) the rod isolated response was borderline normal. The combined rod-cone response had a borderline normal a-wave but the b-wave was selectively moderately reduced. The photopic response and cone response to 30Hz flicker stimulus were moderately reduced with no delay. Taken together this suggests that proband (III:I) has moderate to severe rod and moderate cone dysfunction whilst at the time of examination patient III:II has mild rod dysfunction which is congruent with a cone-rod dystrophy (Fig S4).

Combined with the clinical histories, the sisters appear to have maintained central-most vision until later in the disease course and reported nyctalopia prior to developing the pericentral visual field loss, consistent with earlier compromise of rod rather than cone function. However the pattern was anomalous for typical retinitis pigmentosa. Clinical features such as the sisters exhibited resemble RP spectrum disease and have been described in the literature using terms including retinitis pigmentosa inversa (Ferrucci et al. 1998),

peri-central retinitis pigmentosa (Sandberg et al. 2005), or progressive rod-cone dystrophy (Hartong et al. 2006).

The father of the affected siblings did not manifest this condition, consistent with an autosomal recessive inheritance pattern. He experienced visual symptoms first in his ninth decade of life when he was diagnosed with dry macular degeneration. He showed no retinal pigmentary changes or atrophy beyond the central macula; his visual field was intact with only bilateral central loss mapping to his geographic atrophy, and his optic discs and retinal vasculature appeared normal.

Whole genome sequence analysis:

Sequencing the genomes of both affected siblings and parents of the RF.C.0804 pedigree generated ~900 million to 1,150 million reads in each sample. After duplicates were removed, the mapped reads were estimated to cover the genome at an average depth of 42X;. These reads were utilized to call variants, which identified about 4.5 million variants in each individual including 3.5 million single nucleotide polymorphisms (SNPs) and 1 million insertion-deletions (INDELs). From these, rare variants with a minor allele frequency <0.005 in the 1000 genome project and <0.05 frequency in our in-house WGS dataset of 454 individuals from pedigrees with IRD, a score of deleteriousness by PolyPhen2, high impact variant prediction by SNPEff or a CADD C-score >= 30 were selected for further analysis. This filtering strategy identified 450 to 512 rare and deleterious variants in each of the affected family members. The two affected siblings shared 237 of these rare and potentially pathogenic variants. None of these variants were found to be homozygous. Analysis of the compound heterozygous variants identified only one set of potential disease causing variants, p.Arg266* (c.796C>T, rs145868877) and p.Ala568Thr (c.1702G>A) in the *Intraflagellar transport protein 88* (*IFT88*) (NM_175605) segregating with disease. None of the previously known retinal dystrophy genes were identified to have potential disease causing mutations in affected members of RF.C.0804 pedigree.

Mutation segregation analysis and control individuals screening:

The dideoxy sequencing analysis of variants p.Arg266* (c.796C>T) in exon 13 and p.Ala568Thr (c.1702G>A) in exon 20 of IFT88 demonstrated co-segregation of these variants with disease in RF.C.0804 family (Fig 1.I). The nonsense variant p.Arg266* was found to be heterozygous in the mother and both affected siblings (Fig 1.I). This variant may result in premature truncation of IFT88 leading to the loss of 561 C-terminal amino acids (Fig 1.IV). IFT88 is predicted to have two coiled domains and 10 tetratricopeptide repeat motifs (Fig 1.IV) (Bhogaraju et al. 2013). Therefore, if the p.Arg266* stop gain mutation results in termination of IFT88 at the 266 amino acid, the truncated protein will lose 6 of the 10 tetratricopeptide repeats that are part of the second coiled coil domain. Alternatively, the nonsense variant may result in nonsense mediated decay (NMD) of the transcript, causing the loss of IFT88 protein. The missense variant p.Ala568Thr was observed to be heterozygous in the father and both affected sisters (Fig 1.I) and is located in a highly conserved region of IFT88 (Fig S2). This variant was predicted to be pathogenic by PolyPhen2 (Adzhubei et al. 2013) and SIFT (Hu and Ng 2013) and the presence of this variant may alter the structure of the protein. Structural models indicate the location of

p.Ala568Thr to be in the middle of helix A of a two helix repeat within a larger right-handed super helical fold (Fig S1). The presence of the variant in this location suggests that it could be damaging as a result of the added bulk of the threonine side chain relative to either the adjoining helix B or the adjacent helix A', though the two models evaluated provide conflicting evidence for this hypothesis.

The frequency of both variants c.796C>T (p.Arg266*; ExAC: 0.000009984) and c.1702G>A (p.Ala568Thr; ExAC: 0.00002166) were reported to be very low in the population. Neither of these two variants nor additional damaging variants in *IFT88* were detected in our laboratory WGS database which contained a total of 800 individuals (including 454 individuals from IRD pedigrees). Similarly, the variant data set of a cohort of 150 genetically unexplained inherited retinal disease probands from the Netherlands (Radboudumc, Nijmegen, Netherlands), 618 from Japan and 117 from Pakistan were screened and neither the two potential disease causing variants observed in this study nor additional pathogenic variants were detected in *IFT88*. Furthermore, screening 50 probands of Indian origin and a diagnosis of IRD by dideoxy sequencing also yielded similar findings indicating that the occurrence of pathogenic changes in this gene is not a common event.

Expression and localization of wild type and mutant IFT88 in mIMCD3 cells:

IFT88 is a ciliary protein and is critical for ciliogenesis in a wide variety of sensory cells (Murcia et al. 2000; Pazour et al. 2000). Therefore, to study the effect of p.Arg266* and p.Ala568Thr mutations, ciliated mIMCD3 cells were transiently transfected with GFP tagged wild type-*IFT88* (Fig 2) or Myc tagged Arg266*-*IFT88* (Fig 2) or Myc tagged Ala568Thr-*IFT88* (Fig 2) constructs. An additional set of mock-transfected mIMCD3 cells were analyzed as controls (Fig 2). Cells transfected with wild type-*IFT88*-GFP showed normal ciliary length when stained with acetylated tubulin (Fig 2) and the GFP signal representing the wild type *IFT88* co-localized with the basal body and the distal tip of the cilia as reported earlier (Robert et al. 2007). In contrast, the cells transfected with Arg266*-*IFT88*-Myc or Ala568Thr-*IFT88*-Myc constructs exhibited extra-ciliary localization of the protein (Fig 2). In addition, the length of cilia in cells expressing Myc tagged Arg266*-*IFT88* or Myc tagged Ala568Thr-*IFT88* constructs were found to be significantly shorter ($P<0.0001$) when compared to cells expressing wild type-*IFT88* (Fig 2) indicating defective ciliogenesis in cells expressing *IFT88* mutants. The mock-transfected cells did not show GFP signal or immunostaining with anti-Myc antibodies. The cilia were found to be normal in these cells. These results suggest that both the p.Arg266* and p.Ala568Thr mutations result in mislocalization of IFT88 and abnormal cilia in transiently transfected mammalian cells.

Analysis of the consequences of IFT88 p.Arg266* and p.Ala568Thr mutations:

In order to understand the impact of *IFT88* mutations, p.Arg266* and p.Ala568Thr, the genomes of HeLa cells were edited using CRISPR-Cas9 system. This resulted in the generation of HeLa cells with the homozygous p.Arg266* nonsense mutation and the homozygous p.Ala568Thr missense mutation in IFT88. In addition, a clone with the homozygous p.Arg266Glufs*2 mutation in IFT88 was also identified. All three cell lines were used to study the effect of mutation on IFT88 expression and ciliogenesis. The

p.Arg266* and p.Arg266Glufs*2 mutations located in exon 13 of *IFT88* could result in the formation of a truncated protein or in the loss of IFT88 due to the nonsense mediated decay (NMD) of the transcript. The Arg266*-*IFT88*-Myc construct used for transient transfection studies does not allow the examination of NMD of the mutant transcript. Therefore, the genome edited HeLa cells with the p.Arg266* mutation were studied to examine if the nonsense mutation located in exon 13 resulted in the loss of IFT88 due to NMD. Similarly, the second clone (clone 2) identified with a different stop codon due to the p.Arg266Glufs*2 mutation was also analyzed to further evaluate the impact of nonsense changes in exon 13 of *IFT88*.

To examine the effect of p.Arg266*, p.Arg266Glufs*2 and p.Ala568Thr mutations on cellular morphology and ciliogenesis, the genome edited HeLa cells harboring these mutations and control HeLa cells were stained with the primary cilia marker acetylated alpha tubulin. The majority of normal control HeLa cells (Fig 3A) and a set of HeLa cells treated with transfection reagents (mock transfected - Fig 3B) (>90%) had normal appearing primary cilia as reported previously (Fig 3B) (McIntyre et al. 2012). However, examination of the two independent clones of genome edited HeLa cells harboring the homozygous p.Ala568Thr, p.Arg266* and p.Arg266Glufs*2 mutations revealed that only 15-20% of these cells showed significantly stunted cilia while the remaining cells showed minimal or no ciliary structures (Fig 3, C and D). Similarly, shortened ciliary structure along with mislocalization of IFT88 observed in 40% of the edited cells with p.Ala568Thr mutation (Fig. 3D). But most of the cells (~50%) with p.Ala568Thr mutation were lacking the complete cilia but presence of IFT88 was observed in those cells.

Western blot analysis of the lysates of genome edited HeLa cells harboring homozygous p.Arg266*, p.Arg266Glufs*2 and p.Ala568Thr mutations were carried out to study the IFT88 protein. Immunostaining with IFT88 antibodies raised against the C-terminal region of IFT88 did not detect the presence of protein in either cell line carrying the homozygous nonsense mutations in *IFT88* (Fig 4A, lanes 2 & 4). Whereas, an immune positive band corresponding to wild type IFT88 was observed in the lysates of HeLa cells with the p.Ala568Thr mutation similar to the control and mock transfected HeLa cells (Fig 4A, lanes 1 & 3 and 4 C). The failure to detect an immunoreactive band in the lysates of genome edited cells with the p.Arg266* and p.Arg266Glufs*2 mutations indicated either the absence of mutant protein or the formation of a truncated protein which did not have immunoreactivity to the IFT88 C-terminal region antibodies used.

Analysis of the expression of p.Arg266*-*IFT88* and p.Arg266Glufs*2-*IFT88* transcript:

The *IFT88* transcript levels were measured in HeLa cells with the homozygous mutations p.Arg266* and p.Arg266Glufs*2 in *IFT88* (ENST00000319980.6) and compared with the levels in wild type and mock transfected HeLa cells. The levels of *IFT88* transcript in both cell lines with the *IFT88* mutations were found to be significantly low compared to the levels in wild type and mock transfected cells ($p<0.0001$) (Fig 4B) suggesting that the mutations resulted in the depletion of *IFT88.*

To further study the possible involvement of NMD of the nonsense mutation p.Arg266*, the wild type, mock transfected and the genome edited HeLa cells with the homozygous

p.Arg266* mutation were treated with cycloheximide. No significant difference was observed in the levels of *IFT88* transcript in cycloheximide treated wild type and mock transfected HeLa cells compared to the levels in untreated cells (Fig 5). However, the levels of Arg266*-*IFT88* transcript were found to increase significantly in HeLa cells with the homozygous Arg266*-*IFT88* mutation following cycloheximide treatment (Fig 5). The low levels of mutant transcript and accumulation of this transcript upon treatment with cycloheximide in CRISPR/Cas9 edited HeLa cells with p.Arg266*-*IFT88* mutation suggests the possible involvement of nonsense mediated decay in depletion of this transcript (Durand et al. 2007).

Analysis of off-target effects due to CRISPR-Cas9 genome editing in HeLa cells:

In order to investigate the possible off-target changes introduced into the genomes of HeLa cells with the p.Arg266* and p.Arg266Glufs*2 variants, the off-target sites were identified. This analysis revealed several candidate off-target genomic regions in cells transfected with CRISPR OFP nuclease vector expressing gRNA. Five regions with the highest off-target score were selected for analysis (Table S1). Sanger sequencing confirmed no off-target activity at these potential off-target sites. Therefore the changes observed in these cells are likely due to the homozygous p.Arg266* or p.Arg266Glufs*2 variants in *IFT88*.

DISCUSSION:

Whole genome sequence analysis was conducted on a family with IRD and identified compound heterozygous mutations in *IFT88*, which segregated with retinal degeneration (Fig 1.I). In this family, no other potentially pathogenic mutations were identified in any of the known IRD genes suggesting that the *IFT88* mutations are the likely underlying cause of retinal degeneration.

In photoreceptors, IFTs are responsible for the transport of proteins between the inner and outer segments. Mutations in genes that code for five different IFTs (*IFT172*, *IFT144*, *IFT140*, *IFT43* and *IFT38*) are known to cause human retinal degeneration (Biswas et al. 2017; Bujakowska et al. 2015; Dharmat et al. 2017; Lehman et al. 2008; Xu et al. 2015). The well-established role of IFTs in photoreceptor degeneration and segregation of these novel *IFT88* mutations with IRD in the RF.C.0804 pedigree supports the addition of *IFT88* to the list of IFTs implicated in human disease.

IFT88, one of the well-studied members of the IFT complex, has been considered a candidate gene for human ciliopathy associated phenotypes due to its critical role in cilia and involvement in retinal degeneration and kidney abnormalities in the ORPK mice (Lehman et al. 2008). Targeted screening of *IFT88* for mutations in a cohort of fetuses and individuals with severe ciliopathies identified a homozygous missense variant p.Met383Lys in one fetus of European ancestry with renal and hepatic cysts without polydactyly or encephalocele (McIntyre et al. 2012). This missense variant (p.Met383Lys) was reported to result in the loss of functional IFT88 in a zebrafish model (McIntyre et al. 2012). The frequency of this variant was reported to be very low in individuals of European ancestry (0.000115) while it is more common in the South Asian population (frequency=0.0285) with 10 homozygous individuals listed in the ExAC database. Furthermore, an additional

missense variant, p.Met383Ile (rs2442455), involving the same codon was reported to be a common polymorphism in various populations (ExAC database) indicating that the Methionine at 383 in IFT88 is not critical for the normal function of this protein in humans. Based on these findings it is not clear if the homozygous p.Met383Lys variant in *IFT88* alone is sufficient to cause pathology in the fetus with ciliopathy associated phenotype.

In a more recent study, *IFT88* has been suggested as a candidate gene for autosomal dominant craniofacial abnormalities with variable penetrance (Tian et al. 2017). Review of the clinical data of patients in our study pedigree RF.C.0804 revealed a history of kidney stones in one of the affected siblings (III:I) while the other affected individual lacked any kidney abnormalities. Neither of these patients reported other symptoms associated with ciliopathy. Additionally, evaluation of the clinical history of all members of RF.C.0804 pedigree did not reveal the presence of craniofacial abnormalities or known family history of such abnormalities. It is likely that the two *IFT88* mutations observed in RF.C.0804 pedigree are not associated with non-ocular phenotypes.

Determining the functional impact of the human mutations p.Arg266* and p.Ala568Thr in *IFT88* will reveal the possible mechanism underlying IRD due to these mutations. Mutations in several ciliary proteins affect ciliogenesis and cause severe diseases or embryonic lethality (Cardenas-Rodriguez and Badano 2009). Mouse models for a large number of IFT null alleles are embryonic lethal (McIntyre et al. 2012). In *IFT88*, 53 loss of function alleles are listed in the gnomAD database (accessed on 12-22-17) with a frequency <0.00005. None of the loss of function alleles were reported in the homozygous state in this data base. In addition, pathogenic compound heterozygous mutations have also not been previously reported in patients. These suggest that, severely damaging homozygous or compound heterozygous IFT88 alleles are perhaps embryonic lethal in humans also. In affected members of RF.C.0804 pedigree with *IFT88* compound heterozygous mutations p.Arg266* and p.Ala568Thr, the nonsense mutation may result in the loss of one allele of *IFT88* while the second missense mutation may generate a hypomorphic allele, which may enable to escape developmental abnormalities and embryonic lethality. However, the lack of normal ciliary transport due to the heterozygous p.Ala568Thr mutation in *IFT88* in addition to the depletion of second *IFT88* allele due to the heterozygous p.Arg266* mutation together may lead to photoreceptor degeneration observed in patients by 3rd or 4th decade. Furthermore, these mutations may also have an impact on the non-ciliary functions of *IFT88* contributing to the phenotype. The rare occurrence of the unique set of compound heterozygous variants observed in this study may provide insight into the physiological role of *IFT88* in humans. Additional studies using patient iPSC derived photoreceptor cells or retinal organoid models and mouse models with the p.Arg266* and p.Ala568Thr mutations in *IFT88* may provide a deeper understanding of the mechanism underlying the IRD due to these mutations.

MATERIALS AND METHODS:

Clinical studies:

The family history, medical history and blood samples were collected from the available members (II:I, II:II, III:I and III:II) of family RF.C.0804 (Fig 1(I)). A complete history was obtained from two affected siblings (III:I and III:II) and their father (II:II). Both affected

individuals (III:I and III:II) underwent a complete ophthalmic evaluation which, included fundus photography, kinetic visual fields and visual acuity (VA) measurements as described earlier (Biswas et al. 2016). Full field electroretinograms (ERG) were recorded with corneal electrodes after pupil dilation. Ganzfeld ERGs were performed for brief xenon flash stimuli. After 45-min of dark-adaptation scotopic recordings were performed using dim blue stimuli (−1.82 log cd-s/m^2) and brighter white stimuli (0.83 log cd-s/m^2). After ten minutes of light adaptation to a white 42 cd/m^2 rod saturating background, single flash and 30 Hz flicker ERGs were recorded for white stimuli (0.83 log cd-s/m^2).

All studies on patients were carried out in accordance with the declaration of Helsinki and approval of the Institutional Review Boards of University of California San Diego and the University of Michigan.

Genome data analysis:

DNA was isolated from the blood samples of both affected siblings (III:I and III:II) and their parents (II:I and II:II) using the Qiagen DNeasy kit (Qiagen, Gaithersburg, MD). Whole genome sequencing was performed on the DNA of the four members of the pedigree using the Illumina HiSeq X10 (Illumina, San Diego, CA, USA) to generate 150bp paired end reads at an average read depth of 42x. The following steps were carried out as described previously (Gustafson et al. 2017). Reads were aligned against human genome hg19 and decoy sequences using BWA-MEM, then marked duplicates with Biobambam2 as described previously (Li and Durbin 2009). Single nucleotide variants (SNVs) and insertion deletion variants (INDELs) were called using the Genome Analysis Tool Kit (GATK) best-practice pipeline. SNVs were then annotated using SnpEff, PolyPhen2, and CADD. Structural variants in the genome (SVs) were called with GenomeStrip and SpeedSeq. Variants were filtered to identify rare (<0.005), potentially pathogenic changes in genes expressed in eye tissue and consistent with the pattern of inheritance (Branham et al. 2016).

Mutation segregation analysis and control screening:

Sequence alterations identified as potentially disease-causing variants were validated by dideoxy sequencing in all available members (II:I, II:II, III:I and III:II) of the family as described earlier using the primers listed in Table S1 (Branham et al. 2016). A set of 800 individuals (including 454 individuals from IRD pedigrees and 346 ethnicity matched controls) in our laboratory WGS data set, and the WES data of 150 from Netherlands, 618 from Japan and 117 from Pakistan with IRD were analyzed for *IFT88* mutations using methods described previously (Gustafson et al. 2017).

Designing of *IFT88* constructs:

A GFP tagged wild type *IFT88* construct was purchased from Origene (Rockville, MD) and mutant plasmids were designed in-house for further studies. The p.Ala568Thr (c.1702G>A) missense mutation and nonsense mutation p.Arg266* (c.796C>T) were introduced into the *IFT88* wild type construct using site-directed mutagenesis as described earlier (Biswas et al. 2016). Both constructs were designed to express fusion proteins with a Myc tag at the C terminus in the pCMV6-Entry Mammalian Destination vector and produced by GENEWIZ (GENEWIZ Inc., La Jolla, CA).

Localization of IFT88 protein in transfected cells:

The mIMCD3 cells transfected with the wild type and mutant *IFT88* constructs were collected 48 hours post-transfection, briefly washed in ice cold PBS and fixed with 4% paraformaldehyde. The localization of the mutant IFT88 was detected by immunostaining using anti Myc mAb (1:500) (9B11, Cell Signaling Danvers,MA). Wild type IFT88 was detected by GFP expression. Cilia were stained with acetylated alpha tubulin antibody (Santa Cruz biotechnologies, Dallas, TX) and DAPI (Vector Labs, Burlingame, CA) was used to counterstain nuclei. Images were captured using Nikon confocal microscope system (A1R STORM, Melville, NY, USA). Length of cila was measured using Image J software (NIH USA).

Generation of HeLa cells with p.Arg266*-IFT88 and p.Ala568Thr mutations using CRISPR/Cas9-system:

A gRNA expression vectors were designed to introduce the c.796C>T and c.1702G>A mutations in *IFT88* into HeLa cells by cloning the guide RNA (gRNA) sequences 5'-GAACTTGGTCTAATGCCATT-3' and 5'-ATCTTATTTGAAAACCTTA-3' into a GeneArt CRISPR nuclease vector tagged with an orange fluorescent protein (OFP) (ThermoFisher, Carlsbad, CA) for introducing c.796C>T and c.1702G>A mutations in *IFT88* gene respectively. HeLa cells were transfected with the gRNA expression vector and homology directed repair templates which incorporated a protospacer adjacent motif modified sequences 5'-TATTGTTATAAACTTACCTCATTTGCTTATTGACACTTGGAACTTGGTCTAATGCCATTCaaTAGAATTTAATGGCTTTGGAATAATTTCTTTGCTTTAAATAGATATTTCCCATATTCA-3' and CCTTACCTATGAGAAACTAAATCGGCTAGATGAGGCTTTGGACTGTTTCCTGAAACTTCACGCAATCCTACGAAACAGTGCCGAAGTTCTTTACCAGATAACAAATATGTATCTTATTTGAAAACCTTAGGAACAGTTATTAATTCTCTCAATTGGTGATTGAAGATCAATTATTAAATAAGTTTAACTAATGAAGTAAT for the generation of HeLa cells with c.796C>T and c.1702G>A mutations in *IFT88* respectively (synthesized by Thermo Fisher Scientific, Carlsbad, CA) using lipofectamine 3000 (Thermo Fisher, Carlsbad, CA). Forty-eight hours after transfection, the OFP positive cells were sorted into a 96 well plate with one cell per well using BD FACSAria (BD Biosciences, Franklin Lakes, NJ). Sixty-eight wells were screened for mutations by amplifying and sequencing exon 13 of *IFT88*. One clone (clone 1) with the homozygous p.Arg266* (c.796C>T) mutation was identified. In addition, another clone (Clone 2) with a homozygous c.796delC mutation in *IFT88,* which creates a stop codon (p.Arg266Glufs*2) two amino acids downstream to the p.Arg266*, was identified. Similarly, a clone with the homozygous mutation p.Ala568Thr (1702G>A) in exon 20 of IFT88 was also identified. All three clones were clonally expanded. The presence of the mutations in the homozygous state in *IFT88* exon 13 and 20 were confirmed by amplification and sequencing the DNA from all clones. The expression of Arg266*-IFT88 , Arg266Glufs*2-IFT88 and p.Ala568Thr – IFT88 were studied by western blot analysis of cell lysates using an IFT88 antibody (1:200) (13967-1-AP, Proteintech Group, Inc, Rosemont, IL 60018, USA).

Analysis of CRISPR nuclease vector transfected cells for non-specific changes in the genome:

Genomic regions prone to off-target changes by CRISPR nuclease in the HeLa cell line with the homozygous p.Arg266* *IFT88* mutation were identified by *in silico* analysis using the Cutting Frequency Determination (CFD) score method employing Benchling software (Benchling, San Francisco, CA) (Doench et al. 2016). Regions identified as potential off-target sites were examined for sequence changes by amplification and sequencing as described earlier (Hsu et al. 2013). The primers used for amplification of the selected regions are listed in Table S1.

Analysis of the expression of mutant *IFT88* transcript:

Levels of *IFT88* transcript were studied in control HeLa cells, mock transfected cells expressing the wild type *IFT88* and the cells with the homozygous p.Arg266* and p.Arg266Glufs*2 mutations to understand the impact of mutations resulting in stop codons in exon 13 of *IFT88*. In addition, the HeLa cells (clone 1) with the p.Arg266* human mutation were treated with 100ug/ml cycloheximide (Sigma-Aldrich, Carlsbad CA) followed by incubation in serum containing medium to evaluate the potential involvement of nonsense mediated decay in abrogation of p.Arg266*-*IFT88* (Durand et al. 2007). RNA was isolated from these cells using Qiagen RNeasy Mini Kit (Qiagen, German town MD). Preparation of cDNA using reverse transcriptase and quantitative RT-PCR reaction relative to the housekeeping genes *GAPDH* and *ACTB* were performed as described previously.

Statistical analysis:

Experimental data were represented as means ± standard deviation. Statistical significance was analyzed using students t-test and the p-value less than 0.0001 ($p < 0.0001$) was indicated by *** and determined as statistically significant.

Supplementary Material

Refer to Web version on PubMed Central for supplementary material.

ACKNOWLEDGMENTS:

We are grateful to Dr. Frans Cremers, Department of Human Genetics, Radboud University, for screening his collection of IRD patients for mutations in the *IFT88* gene.

Grants: The Foundation Fighting Blindness, Research to Prevent Blindness, NIH-EY21237, P30-EY22589

REFERENCES

Adzhubei I, Jordan DM, Sunyaev SR (2013) Predicting functional effect of human missense mutations using PolyPhen-2 Curr Protoc Hum Genet 10.1002/0471142905.hg0720s76

Badano JL, Mitsuma N, Beales PL, Katsanis N (2006) The ciliopathies: an emerging class of human genetic disorders Annu Rev Genomics Hum Genet 7:125–148 doi:10.1146/annurev.genom.7.080505.115610 [PubMed: 16722803]

Bhogaraju S, Engel BD, Lorentzen E (2013) Intraflagellar transport complex structure and cargo interactions Cilia 2:10 10.1186/2046-2530-2-10 [PubMed: 23945166]

Bisgrove BW, Yost HJ (2006) The roles of cilia in developmental disorders and disease Development 133:4131–4143 10.1242/dev.02595 [PubMed: 17021045]

Biswas P et al. (2016) A missense mutation in ASRGL1 is involved in causing autosomal recessive retinal degeneration Hum Mol Genet 25:2483–2497 10.1093/hmg/ddw113 [PubMed: 27106100]

Biswas P et al. (2017) A mutation in IFT43 causes non-syndromic recessive retinal degeneration Hum Mol Genet 26:4741–4751 10.1093/hmg/ddx356 [PubMed: 28973684]

Boehlke C et al. (2015) A Cilia Independent Role of Ift88/Polaris during Cell Migration PLoS One 10:e0140378 10.1371/journal.pone.0140378 [PubMed: 26465598]

Branham K et al. (2016) Establishing the involvement of the novel gene AGBL5 in retinitis pigmentosa by whole genome sequencing Physiol Genomics 48:922–927 10.1152/physiolgenomics.00101.2016 [PubMed: 27764769]

Bujakowska KM et al. (2015) Mutations in IFT172 cause isolated retinal degeneration and Bardet-Biedl syndrome Hum Mol Genet 24:230–242 10.1093/hmg/ddu441 [PubMed: 25168386]

Cardenas-Rodriguez M, Badano JL (2009) Ciliary biology: understanding the cellular and genetic basis of human ciliopathies Am J Med Genet C Semin Med Genet 151C:263–280 10.1002/ajmg.c.30227 [PubMed: 19876935]

Chang CF, Serra R (2013) Ift88 regulates Hedgehog signaling, Sfrp5 expression, and beta-catenin activity in post-natal growth plate J Orthop Res 31:350–356 10.1002/jor.22237 [PubMed: 23034798]

Delaval B, Bright A, Lawson ND, Doxsey S (2011) The cilia protein IFT88 is required for spindle orientation in mitosis Nat Cell Biol 13:461–468 10.1038/ncb2202 [PubMed: 21441926]

Dharmat R et al. (2017) IFT81 as a Candidate Gene for Nonsyndromic Retinal Degeneration Invest Ophthalmol Vis Sci 58:2483–2490 10.1167/iovs.16-19133

Doench JG et al. (2016) Optimized sgRNA design to maximize activity and minimize off-target effects of CRISPR-Cas9 Nat Biotechnol 34:184–191 10.1038/nbt.3437 [PubMed: 26780180]

Durand S et al. (2007) Inhibition of nonsense-mediated mRNA decay (NMD) by a new chemical molecule reveals the dynamic of NMD factors in P-bodies J Cell Biol 178:1145–1160 10.1083/jcb.200611086 [PubMed: 17893241]

Ferrucci S, Anderson SF, Townsend JC (1998) Retinitis pigmentosa inversa Optom Vis Sci 75:560–570

Gustafson K et al. (2017) Whole Genome Sequencing Revealed Mutations in Two Independent Genes as the Underlying Cause of Retinal Degeneration in an Ashkenazi Jewish Pedigree Genes (Basel) 8 10.3390/genes8090210

Halbert SA, Patton DL, Zarutskie PW, Soules MR (1997) Function and structure of cilia in the fallopian tube of an infertile woman with Kartagener's syndrome Hum Reprod 12:55–58 [PubMed: 9043902]

Hartong DT, Berson EL, Dryja TP (2006) Retinitis pigmentosa Lancet 368:1795–1809 10.1016/S0140-6736(06)69740-7 [PubMed: 17113430]

Hsu PD et al. (2013) DNA targeting specificity of RNA-guided Cas9 nucleases Nat Biotechnol 31:827–832 10.1038/nbt.2647 [PubMed: 23873081]

Hu J, Ng PC (2013) SIFT Indel: predictions for the functional effects of amino acid insertions/deletions in proteins PLoS One 8:e77940 10.1371/journal.pone.0077940 [PubMed: 24194902]

Katoh Y, Michisaka S, Nozaki S, Funabashi T, Hirano T, Takei R, Nakayama K (2017) Practical method for targeted disruption of cilia-related genes by using CRISPR/Cas9-mediated, homology-independent knock-in system Mol Biol Cell 28:898–906 10.1091/mbc.E17-01-0051 [PubMed: 28179459]

Khanna H (2015) Photoreceptor Sensory Cilium: Traversing the Ciliary Gate Cells 4:674–686 10.3390/cells4040674 [PubMed: 26501325]

Kim S, Tsiokas L (2011) Cilia and cell cycle re-entry: more than a coincidence Cell Cycle 10:2683–2690 10.4161/cc.10.16.17009 [PubMed: 21814045]

Lehman JM, Michaud EJ, Schoeb TR, Aydin-Son Y, Miller M, Yoder BK (2008) The Oak Ridge Polycystic Kidney mouse: modeling ciliopathies of mice and men Dev Dyn 237:1960–1971 10.1002/dvdy.21515 [PubMed: 18366137]

Li H, Durbin R (2009) Fast and accurate short read alignment with Burrows-Wheeler transform Bioinformatics 25:1754–1760 10.1093/bioinformatics/btp324 [PubMed: 19451168]

Liu Q, Zhang Q, Pierce EA (2010) Photoreceptor sensory cilia and inherited retinal degeneration Adv Exp Med Biol 664:223–232 10.1007/978-1-4419-1399-9_26 [PubMed: 20238021]

Marshall WF, Nonaka S (2006) Cilia: tuning in to the cell's antenna Curr Biol 16:R604–614 10.1016/j.cub.2006.07.012 [PubMed: 16890522]

McIntyre JC et al. (2012) Gene therapy rescues cilia defects and restores olfactory function in a mammalian ciliopathy model Nat Med 18:1423–1428 10.1038/nm.2860 [PubMed: 22941275]

Mizuno N, Taschner M, Engel BD, Lorentzen E (2012) Structural studies of ciliary components J Mol Biol 422:163–180 10.1016/j.jmb.2012.05.040 [PubMed: 22683354]

Moyer JH et al. (1994) Candidate gene associated with a mutation causing recessive polycystic kidney disease in mice Science 264:1329–1333 [PubMed: 8191288]

Murcia NS, Richards WG, Yoder BK, Mucenski ML, Dunlap JR, Woychik RP (2000) The Oak Ridge Polycystic Kidney (orpk) disease gene is required for left-right axis determination Development 127:2347–2355 [PubMed: 10804177]

Pazour GJ et al. (2002) The intraflagellar transport protein, IFT88, is essential for vertebrate photoreceptor assembly and maintenance J Cell Biol 157:103–113 10.1083/jcb.200107108 [PubMed: 11916979]

Pazour GJ, Dickert BL, Vucica Y, Seeley ES, Rosenbaum JL, Witman GB, Cole DG (2000) Chlamydomonas IFT88 and its mouse homologue, polycystic kidney disease gene tg737, are required for assembly of cilia and flagella J Cell Biol 151:709–718 [PubMed: 11062270]

Pazour GJ, Rosenbaum JL (2002) Intraflagellar transport and cilia-dependent diseases Trends Cell Biol 12:551–555 [PubMed: 12495842]

Robert A, Margall-Ducos G, Guidotti JE, Bregerie O, Celati C, Brechot C, Desdouets C (2007) The intraflagellar transport component IFT88/polaris is a centrosomal protein regulating G1-S transition in non-ciliated cells J Cell Sci 120:628–637 10.1242/jcs.03366 [PubMed: 17264151]

Rosenbaum J (2002) Intraflagellar transport Curr Biol 12:R125 [PubMed: 11864582]

Rosenbaum JL, Witman GB (2002) Intraflagellar transport Nat Rev Mol Cell Biol 3:813–825 10.1038/nrm952 [PubMed: 12415299]

Sandberg MA, Gaudio AR, Berson EL (2005) Disease course of patients with pericentral retinitis pigmentosa Am J Ophthalmol 140:100–106 10.1016/j.ajo.2005.02.038 [PubMed: 15953579]

Tian H et al. (2017) Intraflagellar transport 88 (IFT88) is crucial for craniofacial development in mice and is a candidate gene for human cleft lip and palate Hum Mol Genet 26:860–872 10.1093/hmg/ddx002 [PubMed: 28069795]

Waters AM, Beales PL (2011) Ciliopathies: an expanding disease spectrum Pediatr Nephrol 26:1039–1056 10.1007/s00467-010-1731-7

Wheway G, Parry DA, Johnson CA (2014) The role of primary cilia in the development and disease of the retina Organogenesis 10:69–85 10.4161/org.26710 [PubMed: 24162842]

Xu M et al. (2015) Mutations in human IFT140 cause non-syndromic retinal degeneration Hum Genet 134:1069–1078 10.1007/s00439-015-1586-x [PubMed: 26216056]

Yoder BK (2007) Role of primary cilia in the pathogenesis of polycystic kidney disease J Am Soc Nephrol 18:1381–1388 10.1681/ASN.2006111215 [PubMed: 17429051]

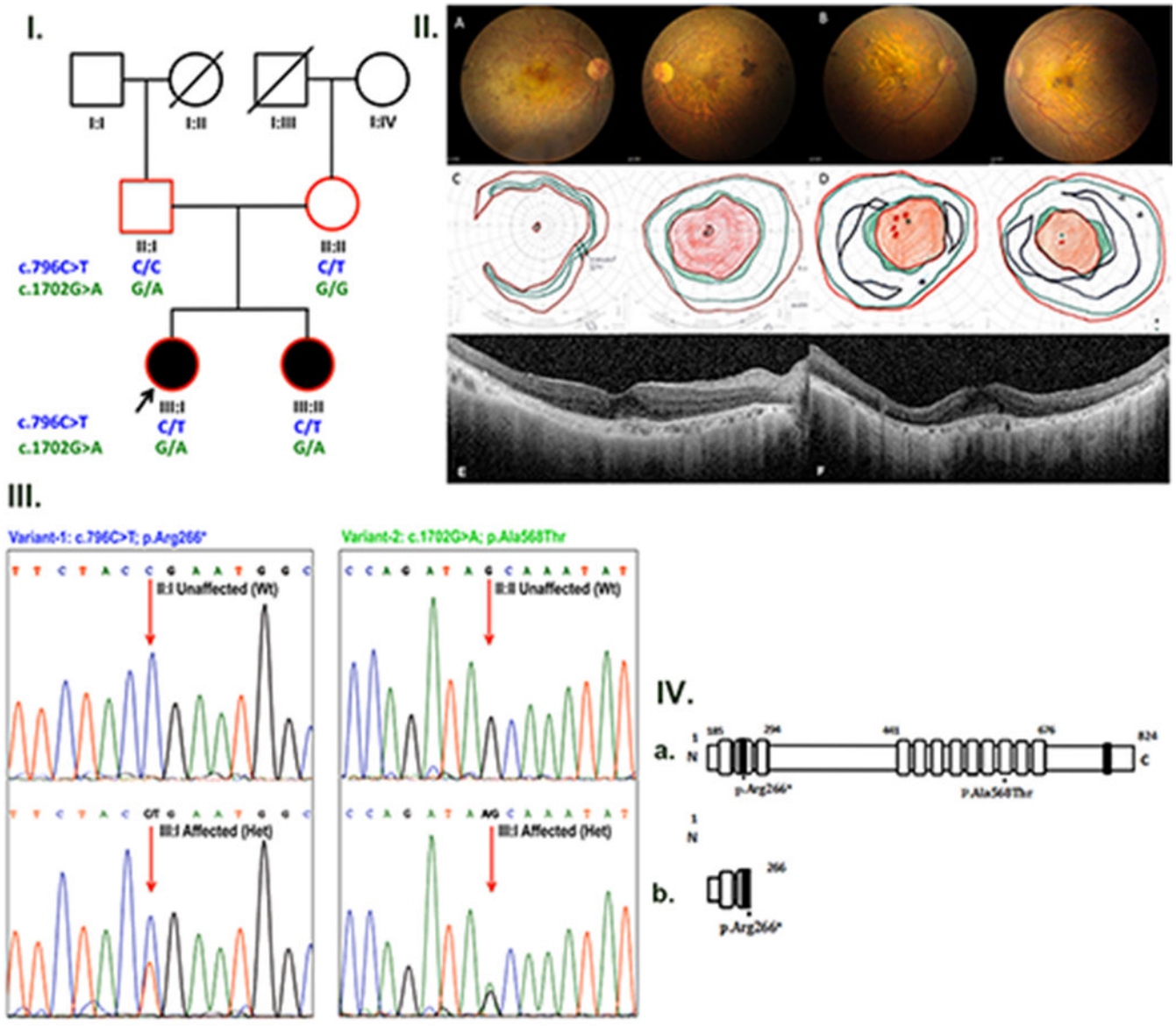

Figure 1.

I. Segregation of *IFT88* compound heterozygous mutations in the pedigree RF.C.0804.

II. Ophthalmic investigations from the two affected individuals. (A and B) Color fundus images form the affected individuals III:I (aged 52) and III:II (aged 47) showing marked macular neuroretinal atrophy with some foveal sparing. There is modest optic disc pallor with mild attenuation of the arcade vascular arcades. Macular and temporal patches of sub-retinal pigment are also identified. (C and D) Kinetic perimetry from the proband III:I (aged 63) and III:II (aged 58) show a dense macular scotoma with minimal foveal sparing. There is relative sparing of visual fields in the far periphery to a Goldman III4e target in both cases. (E and F) SD-OCT cross-section images across the right (E) and left (F) fovea of the III:I (aged 63) show parafoveal and peripheral atrophy of the outer retina with some sparing centrally and nasally in the left eye. Additionally, the choroid appears thinned and atrophic.

III. The sequence of the region containing mutations in *IFT88* exons 13 and 20 in members of RF.C.0804 pedigree. The nucleotides altered are indicated by arrows.

IV. Domain structure of IFT88 with the location of mutations marked. (a) The numbers indicate the amino acid positions. The black boxes represent coiled coil domains whilst gray boxes indicate tetracopeptide repeats (TPR). (b) A truncated protein was predicted to result from the p.Arg266* mutation.

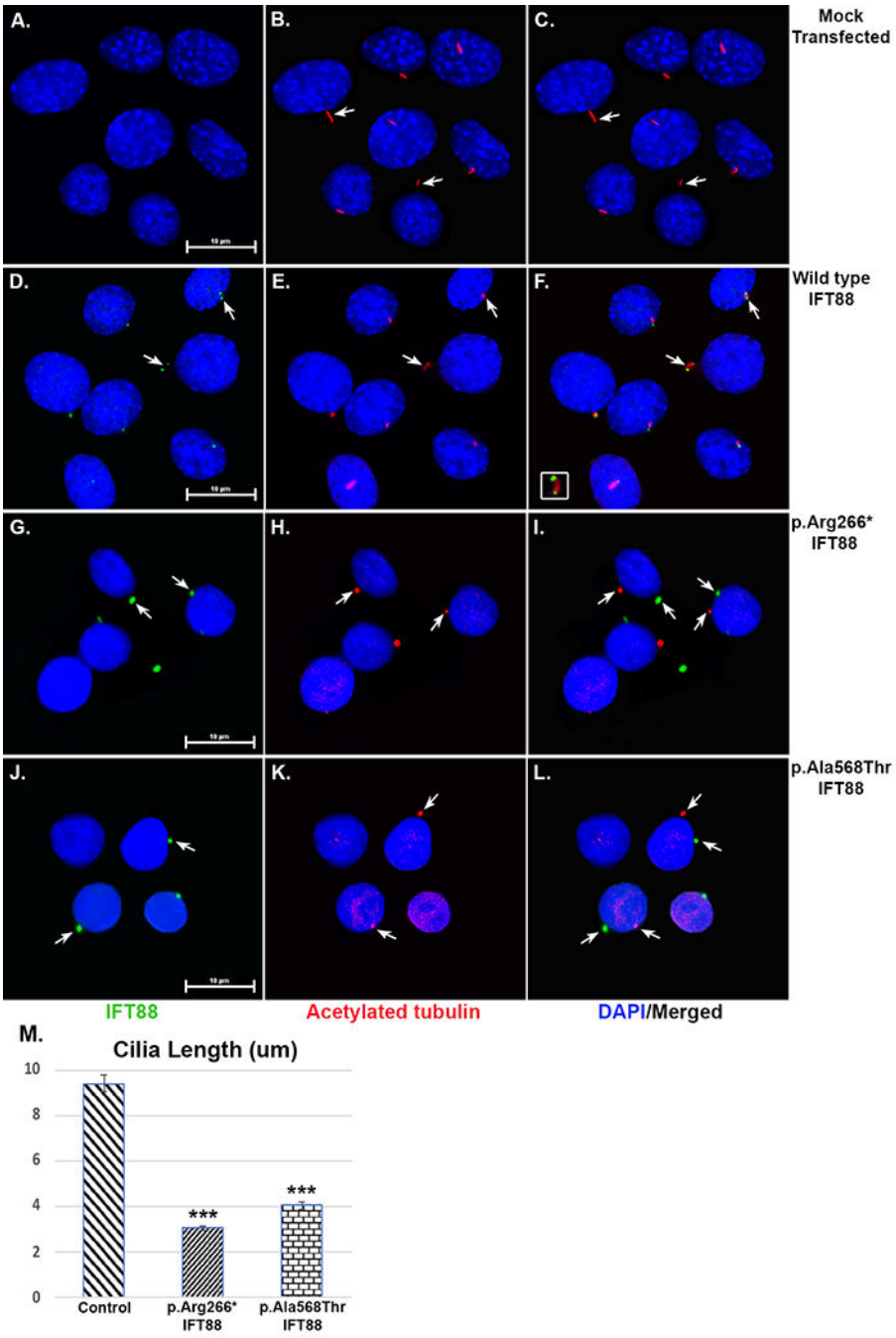

Figure 2. Localization of wild type and mutant IFT88 in transiently transfected mIMCD3 cells.

mIMCD3 cells transiently transfected with wild type IFT88-GFP, p.Arg266* IFT88-Myc and p.Ala568Thr IFT88-Myc were analyzed. Immunostaining was performed with anti Myc antibody (green) and acetylated alpha tubulin (red) a ciliary marker. The nucleus was stained with DAPI (blue). (A-C) Mock transfected HeLa cells were stained acetyl tubulin showed normal cilia. (D-F) Wild type IFT88 (green) was localized to the tip and the base of the cilium (red) (G-I) co-Immunostaining with both acetyl tubulin and IFT88 showed mislocalization of both p.Arg266* IFT88 and (J-L) p.Ala568Thr IFT88 (green) away from

the cilia. (M) Ciliary length of cells expressing wild type IFT88-GFP, p.Arg266* IFT88-Myc and p.Ala568Thr IFT88-Myc were measured using image J (NIH, USA).

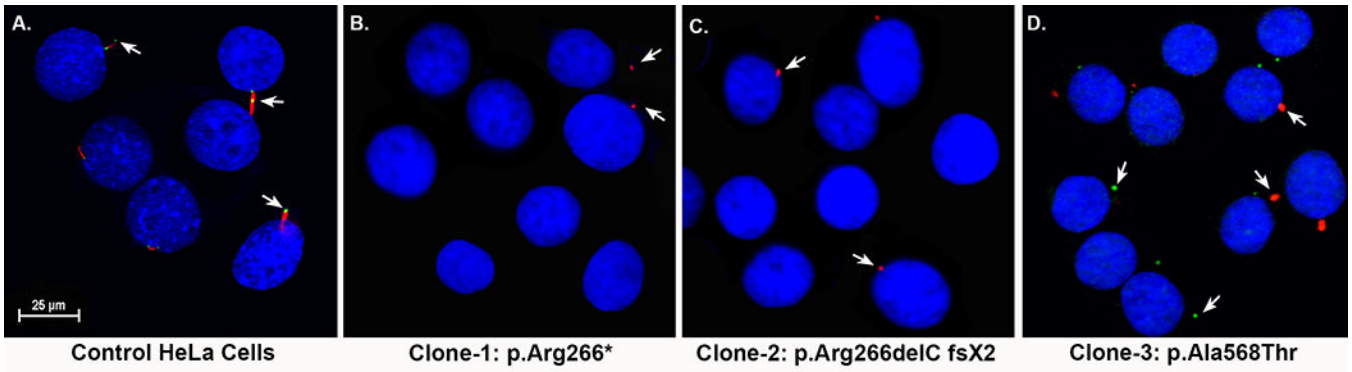

Figure 3. Morphology of cilia in HeLa cell lines with homozygous p.Arg266* and p.Arg266Glufs*2 mutations in *IFT88* introduced using CRISPR-Cas9:

HeLa cells were immunostained for cilia using acetylated alpha tubulin (red). (A & B) Normal appearing cilia (red) were observed in the control and mock transfected HeLa cells. The absence of acetylated alpha tubulin staining or the presence of an abnormal pattern of staining was noted in cells with the homozygous p.Arg266*(Clone 1) (C) and p.Arg266Glufs*2 (Clone 2) (D) *IFT88* mutations.

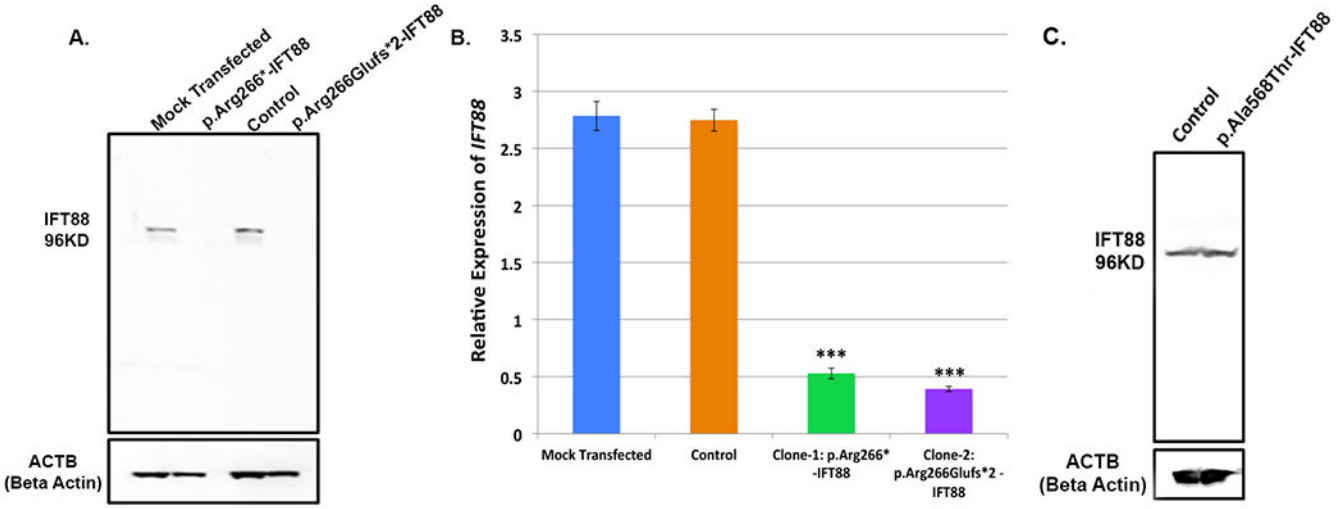

Figure 4.

A. Expression of IFT88 in HeLa cell lines with homozygous p.Arg266* and p.Arg266Glufs*2 mutations. Lysates of mock transfected and control HeLa cells (lane 1 & 3), cells with p.Arg266Glufs*2 (lane 2) and cells with the p.Arg266* mutation (lane 4) were analyzed by western blot analysis using IFT88 antibodies raised against the C-terminal sequence. Presence of expected size IFT88 bands were noted in lanes 1 and 3 while no bands were detected in lanes 2 and 4.

B. Levels of *IFT88* transcript in HeLa cells with the homozygous p.Arg266* and p.Arg266Glufs*2 mutations. qRT-PCR analysis showed the expression of IFT88 transcript in control HeLa cells and mock transfected HeLa cells. Whereas the levels of *IFT88* transcript were significantly low ($P<0.0001$) in both mutant cells lines.

C. Expression of IFT88 in genome edited cells with homozygous p.Ala568Thr mutation. Whole cell lysates of control HeLa cells and and genome edited cells with p.Ala568Thr mutation were analyzed by western blot for expression of IFT88.

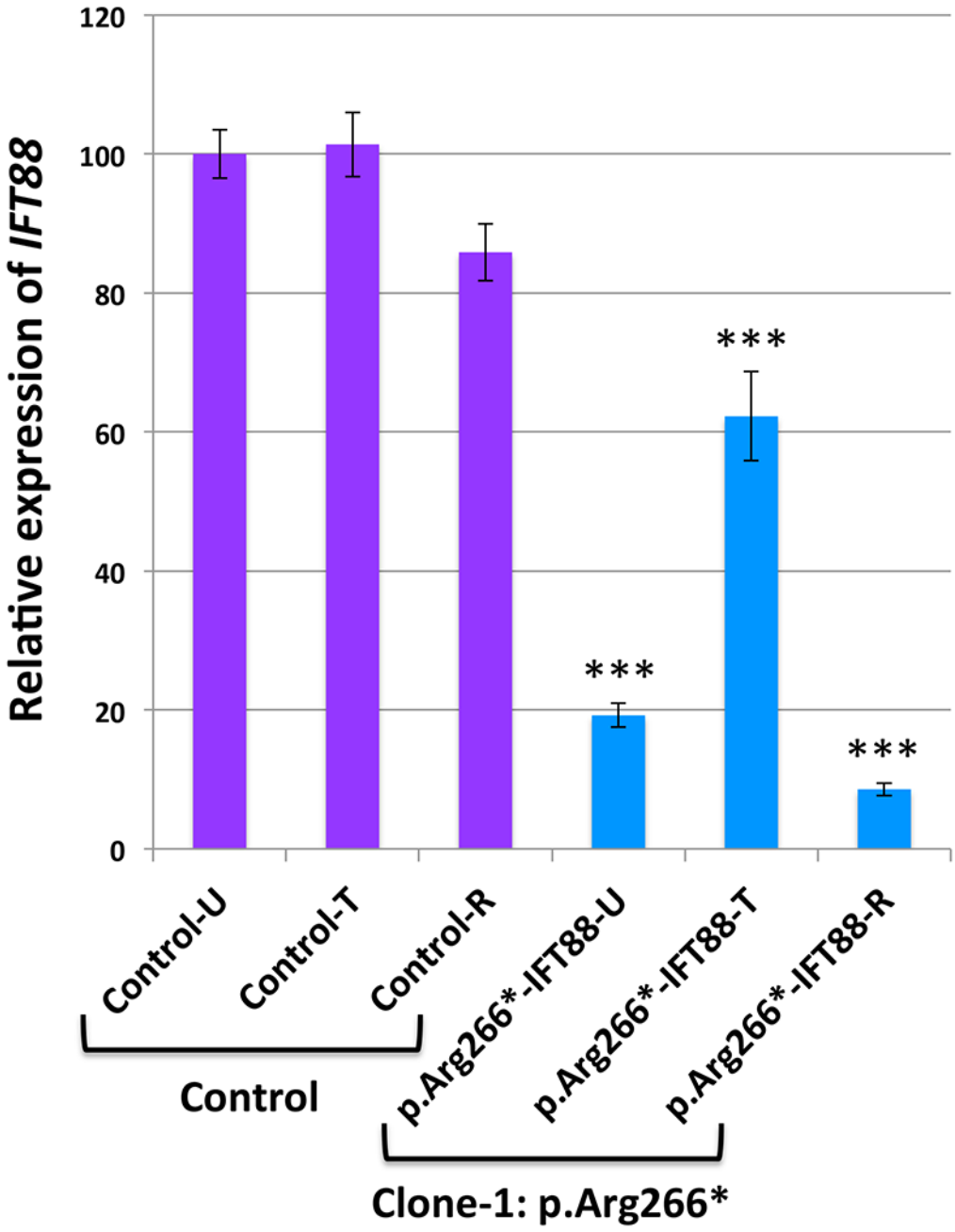

Figure 5. Nonsense-mediated decay of *IFT88* transcript in cells with the homozygous p.Arg266* mutation.

The levels of *IFT88* transcript in mock transfected, control HeLa cells without (*IFT88*-control-U) or with cycloheximide treatment (*IFT88*-control-T) and after recovery (*IFT88*-control-R) were found to be similar. A significant increase in the levels of *IFT88* transcript was observed in response to treatment with cycloheximide in cells carrying the *IFT88* p.Arg266* mutation (*IFT88*-R266*-T) compared to untreated cells (*IFT88*-R266*-U). In these cells, the levels of *IFT88* transcript were found to be significantly lower after recovery

(*IFT88*-R266*-R) compared to the levels observed in cycloheximide treated cells (*IFT88*-R266*-T) (P<0.0001).